Russian Journal of General Chemistry, Vol. 75, No. 5, 2005, pp. 815–824. Translated from Zhurnal Obshchei Khimii, Vol. 75, No. 5, 2005, pp. 863–872.

Synthesis and Steric Structure of H–Leu–His–Lys–Leu–Gln–Thr–NH_2 and H–Ala–*D*-Ala–Lys–Leu–Ala–Thr–NH_2 Peptides

I. V. Rogachevskii*, S. V. Burov, and B. F. Shchegolev***

** Pavlov Institute of Physiology, Russian Academy of Sciences, St. Petersburg, Russia*

*** Institute of Macromolecular Compounds, Russian Academy of Sciences, St. Petersburg, Russia*

Received June 17, 2004

Abstract — Conformational computations of the synthesized H–Leu–His–Lys–Leu–Gln–Thr–NH_2 and H–Ala–*D*-Ala–Lys–Leu–Ala–Thr–NH_2 peptide sequences corresponding to the 16–21 fragment of salmon calcitonin II and its highly active analog that exhibits an analgesic activity were performed. The molecular dynamics method with the AMBER force field was used to trace changes in the geometric parameters of the two molecules over the course of 1500 ps. The conformation of the molecular skeletons underwent no radical changes during computations, and relative flexibility was only revealed in the Lys^3, Leu^4, and Thr^6 side chains.

Development of new approaches to identification of biologically active fragments of natural peptides and proteins is one of the urgent problems of modern bioorganic chemistry. Such compounds may form the basis for preparing analogs possessing selective activity and enhanced resistance to enzymatic cleavage. Analysis of published data shows that α-helix and β-puckered fragments of peptide hormones and proteins not infrequently play an important role in reactions with receptors and cell membranes, as well as function as carriers and antigen determinants. Abundant evidence is available for a correlation between the ability to form such structures and biological activity [1–4], which suggests that search for and study of the corresponding sequence fragments is of independent interest. As one of the objects for such a research we chose salmon calcitonin.

Calcitonin is a peptide hormone comprising 32 amino acid residues. Along with its principal, hypocalcemic function, it controls the concentration of blood phosphorus, exhibits analgesic and anorexic activity, and plays a specific role in stress situations. Despite the fact that human and salmon hormones differ by 16 amino acid residues, salmon calcitonin exhibits a higher affinity for human cell receptors and is 40–50 times more active [5]. Eel calcitonin acts more effectively but for a short time [6]. For this reason, preparations on the basis of salmon calcitonin hold promise as analgesics. At present they are widely used in the therapy of osteoporosis, Paget's disease, and hypercalcemia. Calcitonin is classed with endogenous nonopiate analgesics, and is thoroughly studied [7, 8], in clinics inclusive. It proved very effective against post-amputation pains. At the same time, calcitonin analgesics are frequently unadvisable, since they either directly interfere with the calcium and phosphate metabolism or lead to immune disorders. In this connection, search for elementary hormone units responsible the analgesic activity presents interest.

The analgesic activity of salmon calcitonin fragments has been studied under the direction of G.P. Vlasov at the Institute of Macromolecular Compounds. To gain insight into the nature of the analgesic activity of such compounds, we have synthesized H–Leu–His–Lys–Leu–Gln–Thr–NH_2 and H–Ala–*D*-Ala–Lys–Leu–Ala–Thr–NH_2 peptides which correspond to the 16–21 fragment of salmon calcitonin **II** and its highly active analog, and computed their conformations.

The computations were performed using the HYPERCHEM program package [9]. First geometric parameters of the peptides in the zwitter-ionic form were optimized by molecular mechanics computations with the AMBER force field [10]. Further on the peptide molecules were embraced into solvation shells of water molecules; the latter were treated in terms of the TIP3P model [11]. The hexapeptide molecules with optimized geometric parameters were centered in a parallelepipedic "box"; therewith, the free space was filled with water molecules. The dimensions of the "boxes" were three times the linear dimensions of the H–Leu–His–Lys–Leu–Gln–Thr–NH_2 ($56 \times 35 \times 16$ Å, 1036 water molecules) and H–Ala–*D*-Ala–Lys–

1070-3632/05/7505-0815

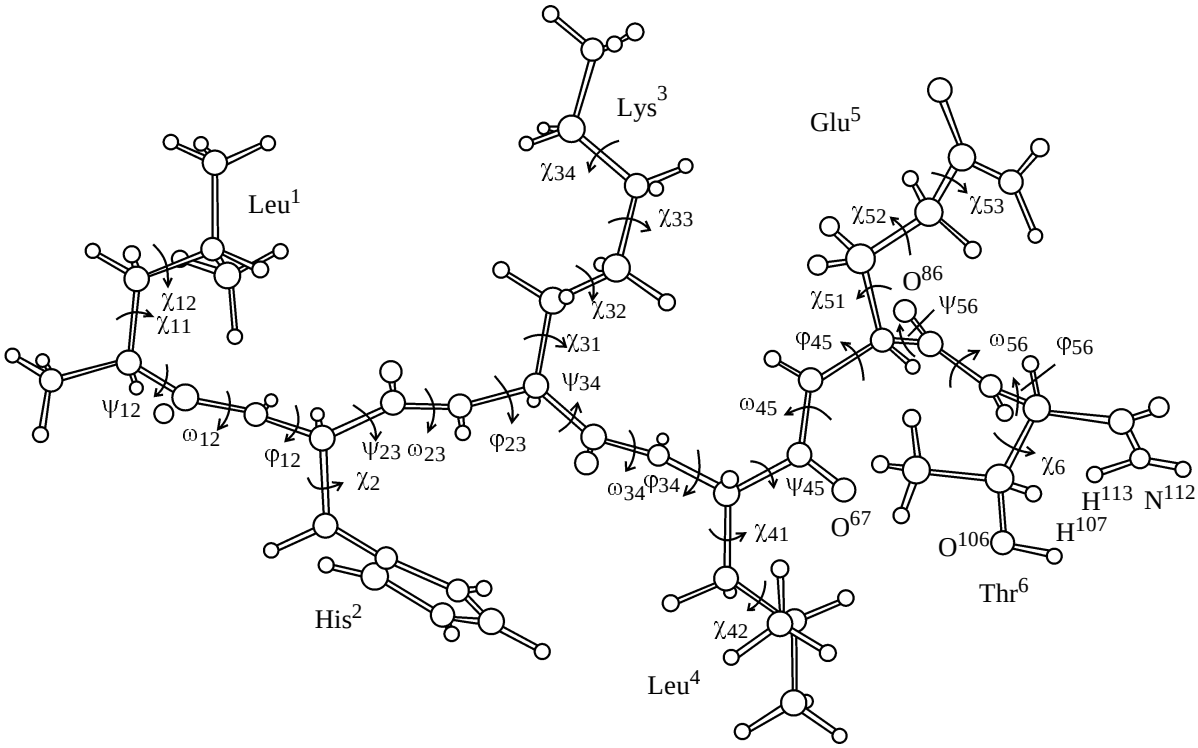

Fig. 1. Spatial arrangement of the lowest energy conformation of the H–Leu–His–Lys–Leu–Gln–Thr–NH_2 molecule in solution and denotations of atoms and dihedral angles.

Leu–Ala–Thr–NH_2 ($56 \times 34.5 \times 19.5$ Å, 1201 water molecules) molecules so as to insulate the peptide molecule from walls of the "box" by a solvent layer and thus prevent boundary effects on the geometry of the peptide during molecular dynamics. Cyclic boundary conditions were imposed on the peptide–solvent system. The whole peptide–water system was optimized by molecular mechanics computations to eliminate energetically unfavorable van der Waals contacts.

The molecular dynamics study of solvated peptides was performed in the following way. Since in the initial conditions the systems were at 0 K, they were first heated to 300 K in 30 steps of 10 K in 30 ps. Further on the total energies of the systems remained roughly constant (while temperature was a computed characteristic related to atomic velocities), and in this state the molecular dynamics was followed up to 1500 ps from the beginning of the computation. The integration step over the entire computation was 0.5 fs. This scheme was preferred over other possible schemes for the following reasons. On the one hand, the temperature was not constant throughout the computation, which allowed the systems to overcome potential barriers higher then they are able to overcome in usual conditions (near 300 K), thus extending potential surfaces available for study. At the same time, the temperature could reach values sufficient for cleavage of covalent bonds or for conformational transitions changing chirality of atoms.

The systems equilibrated 300 ps after the beginning of the experiment, as judged from the ratio of the rms deviation of the total energy to the mean total energy (< 0.0001). Every 10 ps between 1000 to 1500 ps the geometric parameters of the systems were saved (without interrupting molecular dynamics) and optimized by molecular mechanics computations with the AMBER force field, after which the solvent molecules were removed. As a result, 51 conformations for the H–Leu–His–Lys–Leu–Gln–Thr–NH_2 and H–Ala–*D*-Ala–Lys–Leu–Ala–Thr–NH_2 molecules were obtained.

The steric structure of the lowest energy conformation of H–Leu–His–Lys–Leu–Gln–Thr–NH_2 and accepted denotations for geometric parameters are shown in Fig. 1. Dihedral angles were denoted and counted according to the current nomenclature [12]. The optimization results showed that the conformations obtained are expedient to divide into four groups. The structural parameters of the conformations in each group vary only slightly (Table 1). As follows from Table 1, the steric structure of the H–Leu–His–Lys–Leu–Gln–Thr–NH_2 molecular skeleton is almost the same for all the conformations. The most essential

differences in the geometric parameters of the four groups of conformations relate to positions of the Lys, Leu^4, and Thr side chains. Taking as reference second-group conformations, we can infer that first-group conformations have different χ_6 (Thr) angles, third-group conformations, χ_{41} and χ_{42} (Leu^4) dihedral angles, and fourth-group conformations, χ_{33} and χ_{34} (Lys) angles.

By molecular mechanics we additionally optimized all the earlier obtained conformations freed of solvation shells. The desolvated conformations were divided into six groups in terms of potential energies and structural similarity; their geometric parameters are listed in Table 1. The first two groups have dif0 ferent χ_6 angles that define the spatial arrangement of the Thr side chain, but the conformational energies of these groups are roughly close to each other. The principal difference in the geometric parameters between the last four groups and the first two consists in the ψ_{45}, ψ_{56}, and φ_{56} angles: Change in the position of the Gln–Thr fragment relative to Leu–His–Lys–Leu with simultaneous torsion of Thr relative to Gln decreases the conformational energy by ~1–2 kcal mol^{-1}. No other differences in the structure of the peptide skeleton of the last four groups of desolvated conformations and those belonging to the first two groups were revealed; different are only the

Table 1. Geometric parameters of solvated (solv) and desolvated (desolv) conformations and trajectory-averaged (dyn) geometric parameters of the H–Leu–His–Lys–Leu–Gln–Thr–NH_2 molecule: number of conformations in group (N_{conf}), dihedral angles (ψ_{12}, ω_{12}, φ_{12}, ψ_{23}, ω_{23}, φ_{23}, ψ_{34}, ω_{34}, φ_{34}, ψ_{45}, ω_{45}, φ_{45}, ψ_{56}, ω_{56}, φ_{56}, χ_{11}, χ_{12}, χ_2, χ_{31}, χ_{32}, χ_{33}, χ_{34}, χ_{41}, χ_{42}, χ_{51}, χ_{52}, χ_{53}, χ_6, deg), and scatter of potential energies within group (E_{pot}, kcal mol^{-1}), as given by molecular dynamics computations

Parameter	solv				desolv	
	N_{conf} 22	N_{conf} 20	N_{conf} 5	N_{conf} 4	N_{conf} 12	N_{conf} 7
ψ_{12}	152.3±4.6	154.0±2.4	152.1±4.2	153.3±2.0	158.0±1.1	157.9±1.5
ω_{12}	175.3±2.8	175.2±2.1	174.4±3.3	174.4±3.3	169.2±0.5	168.9±0.9
φ_{12}	152.3±4.6	154.0±2.4	152.1±4.2	152.1±4.2	–165.6±1.2	–165.2±1.4
ψ_{23}	168.7±3.4	165.7±3.8	167.6±4.6	167.6±4.6	177.5±1.9	177.1±1.7
ω_{23}	172.1±3.9	171.8±2.1	172.5±2.6	172.5±2.6	175.6±1.2	175.7±1.0
φ_{23}	–147.6±5.3	–142.4±5.4	–145.8±4.6	–145.8±4.6	–162.6±3.6	–160.7±4.4
ψ_{34}	153.8±3.0	150.7±3.5	148.6±3.2	148.6±3.2	172.8±2.4	172.0±3.0
ω_{34}	168.7±2.3	168.3±2.8	170.4±1.1	170.4±1.1	154.9±1.6	156.5±2.1
φ_{34}	–144.3±3.1	–140.5±3.8	–139.2±2.0	–139.2±2.0	–119.4±4.0	–120.1±2.2
ψ_{45}	59.3±3.4	65.5±4.7	69.7±3.9	69.7±3.9	142.3±4.3	142.3±3.0
ω_{45}	161.1±3.8	167.1±2.7	166.6±4.9	166.6±4.9	175.5±1.4	177.0±1.4
φ_{45}	–80.1±4.0	–91.4±6.8	–98.9±1.5	–98.9±1.5	–157.7±2.2	–157.5±0.9
ψ_{56}	118.1±4.8	106.5±4.1	104.5±4.8	104.5±4.8	77.9±3.9	77.8±2.0
ω_{56}	–161.1±3.8	–171.4±2.1	–172.1±6.1	–172.1±6.1	–175.0±1.6	–176.3±1.6
φ_{56}	–166.4±10.1	–145.5±3.4	–139.9±5.0	–139.9±5.0	–138.0±3.2	–129.8±2.2
χ_{11}	–175.4±2.8	–175.9±2.6	–174.4±3.7	–173.4±2.9	–175.5±0.9	–175.7±0.5
χ_{12}	–172.6±3.4	–175.9±1.8	–176.5±3.0	–175.8±3.6	179.1±0.6	–179.0±0.6
χ_2	–175.0±2.1	–173.7±3.2	–173.3±2.7	–170.2±1.5	–164.8±1.6	–163.9±1.6
χ_{31}	–165.1±2.6	–163.9±2.2	–162.9±1.6	–166.0±2.7	–150.8±2.4	–153.3±2.8
χ_{32}	175.7±1.6	174.3±2.7	176.0±1.1	–172.8±2.1	–175.0±2.8	–175.1±2.8
χ_{33}	–175.6±3.6	–175.1±3.3	–176.4±0.8	–63.4±3.2	176.9±1.7	177.7±1.8
χ_{34}	177.5±2.3	176.1±3.0	177.3±2.7	–168.1±3.1	177.9±0.9	–179.2±0.2
χ_{41}	–173.4±5.1	–170.4±2.6	–162.0±2.9	–173.8±4.0	177.0±2.0	179.0±0.4
χ_{42}	–171.6±6.8	–167.3±7.4	–83.0±6.5	–166.5±7.8	–175.3±1.3	–173.4±2.2
χ_{51}	–165.0±5.3	–168.5±2.2	–166.5±2.7	–168.0±4.5	–170.1±1.4	–170.6±1.1
χ_{52}	–111.1±8.9	–110.5±5.9	–108.6±2.6	–105.0±4.4	166.4±2.3	167.0±1.9
χ_{53}	70.3±11.4	63.3±9.9	61.9±11.1	72.7±14.6	121.1±3.5	120.8±1.7
χ_6	158.8±4.0	–64.3±6.3	–59.6±4.0	–67.2±8.6	–178.1±1.7	–67.8±1.1
E_{pot}	–16.31 to –25.17	–17.99 to –25.44	–18.60 to –24.32	–19.50 to 28.21	–66.38 to –66.65	–66.55 to –66.85

Table 1. (Contd.)

Parameter	desolv				dyn
	N_{conf} 4	N_{conf} 4	N_{conf} 10	N_{conf} 4	
ψ_{12}	159.4 ± 0.4	159.2 ± 0.3	159.0 ± 0.7	159.5 ± 0.5	157.0 ± 8.8
ω_{12}	168.0 ± 0.2	164.1 ± 0.6	165.8 ± 0.7	165.6 ± 0.9	172.5 ± 5.0
φ_{12}	–161.6 ± 1.8	–159.3 ± 0.9	–158.3 ± 1.2	–158.2 ± 1.1	–151.0 ± 12.2
ψ_{23}	172.0 ± 1.8	–178.1 ± 0.5	169.3 ± 1.0	171.6 ± 1.1	–143.2 ± 9.6
ω_{23}	172.7 ± 0.3	170.7 ± 0.9	171.6 ± 0.5	170.2 ± 0.5	171.9 ± 5.1
φ_{23}	–154.6 ± 0.4	–164.5 ± 0.6	–154.1 ± 0.6	–153.7 ± 0.5	–143.2 ± 9.6
ψ_{34}	174.7 ± 1.7	174.8 ± 0.5	176.9 ± 0.8	177.1 ± 0.7	149.8 ± 7.5
ω_{34}	161.6 ± 0.6	169.5 ± 0.3	162.2 ± 1.4	162.4 ± 0.8	170.3 ± 5.6
φ_{34}	–136.0 ± 0.4	–146.6 ± 0.3	–139.3 ± 1.0	–139.6 ± 0.8	–140.2 ± 8.3
ψ_{45}	51.9 ± 3.0	53.3 ± 0.8	49.5 ± 1.1	48.6 ± 1.4	60.8 ± 9.8
ω_{45}	171.2 ± 0.2	–177.5 ± 0.4	–174.5 ± 0.9	–174.7 ± 0.2	163.0 ± 7.1
φ_{45}	–158.6 ± 1.2	–162.2 ± 1.5	–157.8 ± 1.5	–156.9 ± 1.7	–80.9 ± 12.9
ψ_{56}	104.6 ± 5.1	116.7 ± 1.5	108.3 ± 1.4	109.0 ± 3.1	116.4 ± 11.6
ω_{56}	175.8 ± 1.2	174.7 ± 1.1	175.4 ± 1.2	176.0 ± 1.8	–166.6 ± 8.2
φ_{56}	–68.5 ± 1.6	–72.9 ± 1.6	–74.0 ± 3.1	–72.1 ± 3.5	–149.1 ± 14.0
χ_{11}	–117.0 ± 0.4	–177.8 ± 1.1	–178.0 ± 0.7	–178.3 ± 0.5	–170.9 ± 5.9
χ_{12}	–178.6 ± 0.5	–177.9 ± 1.7	–178.4 ± 0.7	–178.0 ± 0.7	–171.7 ± 5.9
χ_{2}	–163.9 ± 1.1	–162.9 ± 0.6	–166.2 ± 1.5	–164.4 ± 1.2	–172.1 ± 5.3
χ_{31}	–74.1 ± 3.4	–148.8 ± 1.5	–72.6 ± 1.1	–71.9 ± 1.4	–162.4 ± 7.8
χ_{32}	–167.4 ± 2.7	172.7 ± 1.8	–167.9 ± 1.0	–168.3 ± 1.1	180 ± 10
χ_{33}	169.7 ± 3.7	–63.4 ± 1.4	172.7 ± 1.2	172.7 ± 0.6	–
χ_{34}	–175.3 ± 3.2	–169.2 ± 1.8	179.0 ± 0.6	–178.8 ± 0.8	180 ± 10
χ_{41}	–151.2 ± 0.6	–171.4 ± 0.3	–171.6 ± 1.4	–169.6 ± 1.8	–169.1 ± 6.1
χ_{42}	–61.3 ± 0.4	–177.9 ± 1.8	–176.7 ± 2.6	–174.7 ± 3.5	–
χ_{51}	179.2 ± 0.8	170.5 ± 0.1	177.3 ± 0.7	177.2 ± 0.3	–166.7 ± 7.8
χ_{52}	–90.8 ± 1.6	–92.1 ± 0.8	–89.2 ± 1.8	–89.4 ± 1.3	–
χ_{53}	141.6 ± 4.8	159.4 ± 1.6	145.2 ± 2.3	145.8 ± 2.3	–
χ_{6}	–65.8 ± 1.5	–68.0 ± 1.7	–67.0 ± 1.1	–177.8 ± 1.1	–
E_{pot}	–67.31 to –67.80	–67.48 to –67.55	–68.51 to –69.01	–68.82 to –68.93	–

dihedral angles that define the spatial arrangement of side chains in H–Leu–His–Lys–Leu–Gln–Thr–NH_2, namely, χ_{11} (Leu[1]), χ_{31} (Lys), $\chi_{41,}$ and χ_{42} (Leu[4]) in the third group, $\chi_{31,}$ $\chi_{32,}$ and χ_{33} (Lys) in the fourth, and χ_{31} (Lys) in the fifth and sixth. Fifth- and sixth-group conformations have different χ_6 (Thr) dihedral angles. In Table 1 we included data for 41 desolvated conformations only, since after optimization we obtained six conformations having an appreciably higher energy (by ~4–6 kcal mol^{-1}) and strongly differing in geometry both from each other and from conformations placed in the above groups. Four more conformations, by contrast, had a much lower energy (by ~10–15 kcal mol^{-1}) and an intramolecular hydrogen bond between the nitrogen atom of the Lys side chain and the amide oxygen atom of Gln (N–O distance 2.65–2.75 Å).

As follows from a comparison of the geometric parameters of solvated and desolvated conformations of the H–Leu–His–Lys–Leu–Gln–Thr–NH_2 molecule, solvent has almost no effect on the steric structure of the Leu[1]–His fragment but appreciably affects the structural parameters of the Lys, Gln, and Thr side chains, as well as of the peptide skeleton in the Leu[4]–Gln–Thr region. A probable explanation consists in that the Leu[1]–His fragment is hydrophobic, while the Lys–Leu[4]–Gln–Thr fragment comprises the protonated amino group of the Lys side chain, the hydroxy group of the Thr side chain, and the amido groups of the Gln side chain and peptide C terminus.

We traced the geometric parameters of the H–Leu–His–Lys–Leu–Gln–Thr–NH_2 molecule directly over the course of molecular dynamics simulation in the

range 300–1500 ps at 2-fs steps. The parameter set included all skeleton and side-chain dihedral angles, except for the dihedral angles in the histidine imidazole ring, as well as certain N–O distances. Table 1 lists the trajectory-averaged geometric parameters of H–Leu–His–Lys–Leu–Gln–Thr–NH_2. Most of them only slightly vary with time. Relatively larger variations are only characteristic of χ_{33}, χ_{42}, χ_{52}, χ_{53}, and χ_6. Figure 2 shows χ_{52}, χ_{53}, and χ_6 as functions of computation time. The χ_{52} value fluctuates within

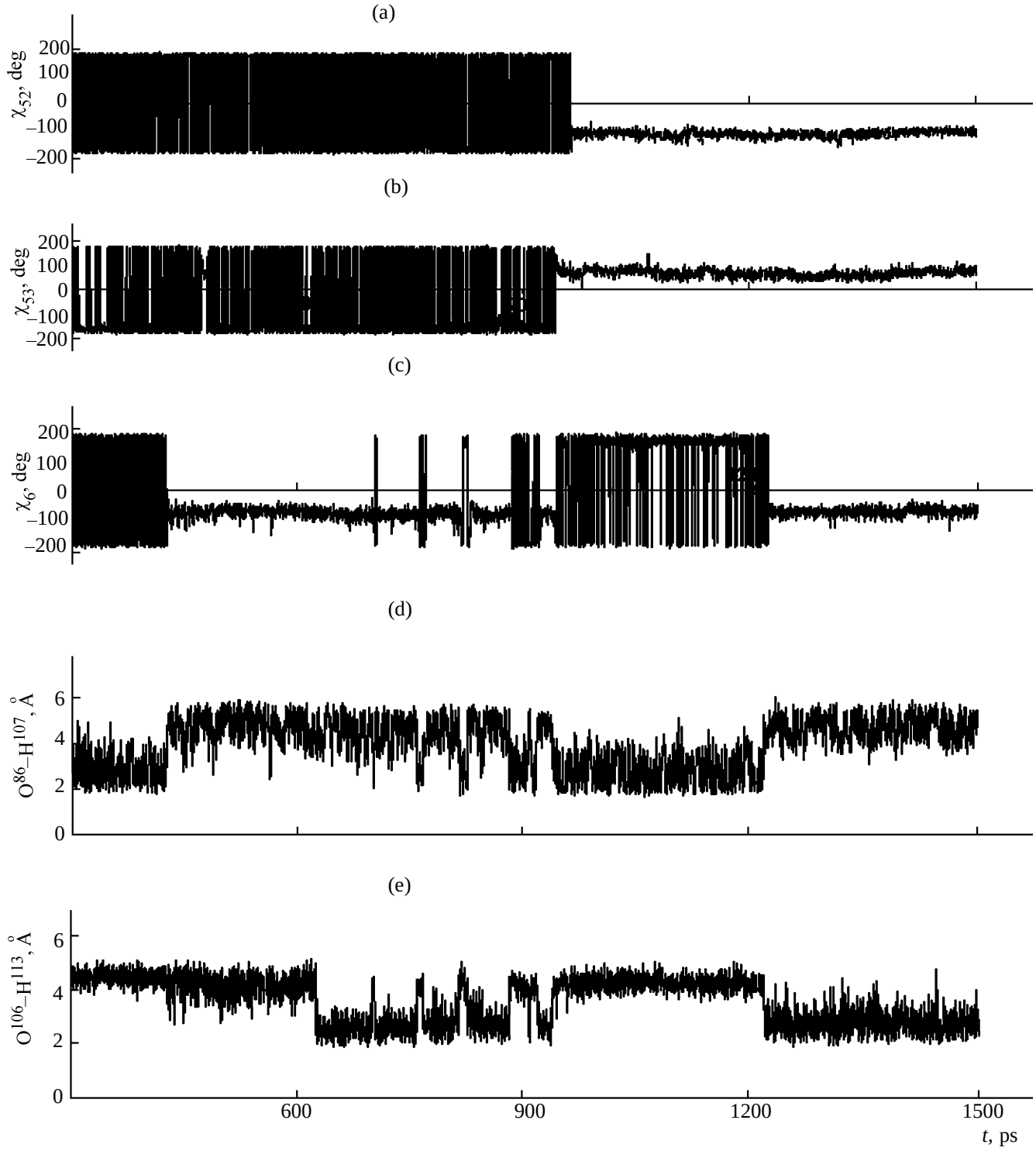

Fig. 2. Dependence of the (a–c) χ_{52}, χ_{53}, and χ_6 dihedral angles and (d, e) O^{86}–H^{107} and O^{106}–H^{113} distances in the H–Leu–His–Lys–Leu–Gln–Thr–NH_2 molecule on the time of molecular dynamics computations (*t*, ps).

Table 2. Dependence of selected O–N, O–H, O–N, and N–H distances (Å) on computation time (*t*, ps)

t	O^{86}–O^{106}	O^{86}–H^{107}	O^{106}–N^{112}	N^{112}–H^{107}	O^{106}–H^{113}
300±425	2.99±0.24	2.98±0.63	4.57±0.14	4.89±0.31	4.30±0.37
425±624	4.33±0.30	4.66±0.61	3.91±0.31	4.06±0.32	2.48±0.23
624±757	–	–	3.05±0.19	3.18±0.34	–
757±765	3.05±0.23	2.65±0.37	4.34±0.15	4.61±0.24	4.04±0.24
765±812	4.28±0.27	4.50±0.56	3.08±0.16	3.28±0.37	2.43±0.27
812±824	2.84±0.20	2.85±0.61	4.42±0.21	4.81±0.20	4.16±0.36
824±880	4.37±0.31	4.72±0.59	3.12±0.19	3.20±0.28	2.47±0.20
880±916	2.91±0.19	2.67±0.40	4.32±0.24	4.68±0.26	4.20±0.37
916±936	4.24±0.27	4.82±0.37	3.11±0.22	2.85±0.30	2.51±0.25
936±1215	2.88±0.22	2.72±0.59	4.43±0.15	4.77±0.26	4.20±0.35
1215±1500	4.51±0.23	4.70±0.51	3.12±0.23	3.10±0.28	2.58±0.27

180°±15° up to 963 ps, after which it is –110.6°± 10.8°. The χ_{53} and χ_{33} values behave similarly: 69.5± 15.6° after 928 ps, –72.3±11.6° after 425 ps, and –68.3°±13.0° after 1464 ps, respectively. The χ_{42} dihedral angle is mostly within 180°±15°, but in the ranges 1248–1264 and 1417–1449 ps it takes the value of –78.6°±11.2°. The χ_6 dihedral angle is within 180°± 15°, except for the ranges 425–880 and 916–936 ps, where it is –72.3°±11.6 and –76.3°±14.2°, respectively. After 1215 ps, this parameter takes the value of –67.6°±11.8°.

We also studied the possibility of intramolecular hydrogen bonding. As heavy atoms potentially capable of hydrogen bonding we considered the hydroxyl O^{106} atoms of the Thr side chain, the peptide carbonyl O^{86} and O^{67} atoms of Leu^4 and Gln, and the N^{112} atom of the N terminus. We traced the O^{67}–O^{106}, O^{67}–H^{107}, O^{86}–O^{106}, O^{86}–H^{107}, O^{106}–N^{112}, N^{112}–H^{107}, and O^{106}–H^{113} distances (Fig. 1). The O^{67}–O^{106} and O^{67}–H^{107} distances vary only slightly: Their mean values in the range 300–1500 ps are 3.98±0.47 and 3.97±0.52 Å, respectively, which rules out formation of an O^{106}–$H^{107}\cdots O^{67}$ hydrogen bond. The dynamics of variation in the other distances is presented in Table 2. The time dependences of the O^{86}–H^{107} and O^{106}–H^{113} distances are shown in Fig. 2.

As seen from Table 2, there is no time range where a hydrogen bond involving O^{106} in the H–Leu–His–Lys–Leu–Gln–Thr–NH_2 molecule would persist over the entire interval, since the O^{86}–H^{107}, N^{112}–H^{107}, and O^{106}–H^{113} distances are too large. However, in certain conformations, the O^{106}–$H^{107}\cdots O^{86}$ and O^{106}–$H^{113}\cdots N^{112}$ hydrogen bonds were found. It is also seen that the processes of $H^{107}\cdots O^{86}$ and O^{106}–$H^{113}\cdots N^{112}$ bond formation are competitive: The H–Leu–His–Lys–Leu–Gln–Thr–NH_2 molecule never contains both these bonds together.

According to the computation results, no radical changes in the H–Leu–His–Lys–Leu–Gln–Thr–NH_2 molecular conformation occur during molecular dynamics up to 1500 ps; the geometric parameters averaged over the molecular dynamics trajectory and a series of lowest energy conformations vary only slightly. Therefore, it is safe to state that the molecular dynamics trajectory of solvated H–Leu–His–Lys–Leu–Gln–Thr–NH_2 passes near minima on the peptide–solvent potential energy surface.

The spatial arrangement and accepted denotations for geometric parameters of the H–Ala–*D*-Ala–Lys–Leu–Ala–Thr–NH_2 molecule are presented in Fig. 3. The conformations are divided into four groups with close dihedral angles (Table 3). The structure of the molecular skeleton is almost the same in all the conformations, and different is only the spatial arrangement of the Lys and Leu side chains. For the Ala–*D*-Ala–Lys–Leu–Ala–Thr–NH_2 molecule, too, additional optimization of desolvated conformations was performed to assess the effect of solvation on the peptide geometry. The dihedral angles for five groups of desolvated conformations are given in Table 3.

The first and fourth groups radically differ from the other three in the structure of the peptide skeleton, as evidenced by the magnitudes of the φ_{12}, φ_{23}, Ψ_{34}, ω_{34}, φ_{34}, and χ_{31} dihedral angles. The first group differs from the fourth and the second, third, and fifth groups differ from each other in the structure of the Lys and Leu side chains. The torsion by ~90° (χ_{42}) of the 2-propyl substituent in the Leu side chain decreases the conformational energy by ~1.5–2 kcal mol^{-1} (difference between the second and third groups), and further changes in the structure of the Lys side (decrease by ~120° of the χ_{33} and χ_{34} dihedral angles), decreases the energy by almost the same value (difference between the third and fifth

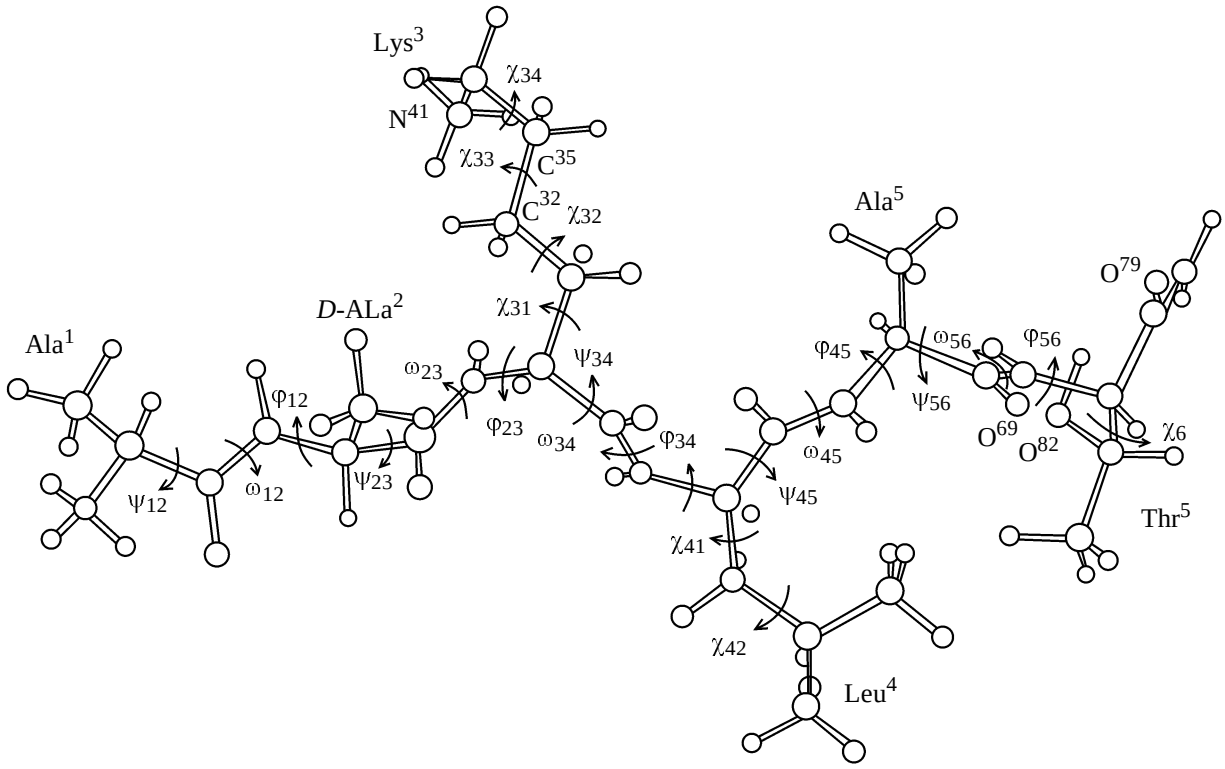

Fig. 3. Spatial arrangement of the lowest energy conformation of the H–Ala–*D*-Ala–Lys–Leu–Ala–Thr–NH_2 molecule in solution and accepted denotations for atoms and dihedral angles.

groups). Table 3 gives no data for four desolvated conformations that have much lower (100–110 kcal mol^{-1}) energies compared to the other conformations. These conformations are stabilized by N–H···O intramolecular hydrogen bonds between the amino N^{41} atom of the Lys side chain and oxygen atoms: O^{79} of the C-terminal amido group and two of the three atoms O^{50} and O^{69} (peptide carbonyls of Leu and Ala^5, respectively) (Fig. 3).

Analysis of the molecular dynamics trajectory of H–Ala–*D*-Ala–Lys–Leu–Ala–Thr–NH_2 in the range 300–1500 ps revealed no changes in the skeletal conformation. The trajectory-averaged dihedral angles are listed in Table 3. Conformational transitions occur exclusively in the Lys and Leu side chains; Fig. 4 show χ_{33}, χ_{34}, and χ_{42} as functions of computation time. At 857 ps, torsion about the C^{32}–C^{35} bond occurs, which changes the χ_{33} angle (87.9° ± 9.8° at 300–857 ps and 137.4° ± 10.4° at 857–1068 ps). At 1068 ps, concerted changes in χ_{33} and χ_{34} are observed: χ_{33} fluctuates within 180 ± 20° at 1068–1500 ps, and χ_{34} is 71.5° ± 9.2° at 300–1068 ps and –57.5° ± 9.7° at 1068–1500 ps. The χ_{42} value exhibits the most unstable behavior: It varies within 180° ± 25° at 300–631, 637–644, 653–832, and 865–1035 ps, and –101.9° ± 8.2, –99.0° ± 8.1, –89.3° ± 16.1, and –73.4° ± 7.2° at 631–637, 644–653, 832–865, and 1035–1500 ps, respectively. The χ_{41} value fluctuates within 180° ± 25° at 300–865 ps and are 169.5° ± 6.2, and –164.4° ± 8.3° at 865° ± 1035, and 1035 ± 1500 ps, respectively.

Preliminary experiments in rats (Formalin test) showed that the peptide molecules in hand exhibit expressed analgesic activity. The analgesic activity of salmon calcitonin was also revealed by means hot plate and clipping tests. It was also established that the analgesic effect is not relieved with naloxone, a specific opiate antagonist [13]. At the same, the mechanism of the analgesic activity both of calcitonin itself and of its shortened analogs is still unclear.

Probably, H–Leu–His–Lys–Leu–Gln–Thr–NH_2 and H–Ala–*D*-Ala–Lys–Leu–Ala–Thr–NH_2 selectively interact with certain membrane receptors. Our computations show that such ligand–receptor interaction can be realized via formation of a hydrogen bond involving one or several functional groups. Both molecules have common Lys^3, Leu^4, and Thr^6 residues. The Leu^4 side chain is hydrophobic and contains no atoms capable of hydrogen bonding. Consequently, the groups responsible for ligand–acceptor binding are

Table 3. Geometric parameters of solvated (solv) and desolvated (desolv) conformations and trajectory-averaged (dyn) geometric parameters of the H–Ala–*D*-Ala–Lys–Leu–Ala–Thr–NH_2 molecule: number of conformations in group (N_{conf}), dihedral angles (ψ_{12}, ω_{12}, φ_{12}, ψ_{23}, ω_{23}, φ_{23}, ψ_{34}, ω_{34}, φ_{34}, ψ_{45}, ω_{45}, φ_{45}, ψ_{56}, ω_{56}, φ_{56}, χ_{31}, χ_{32}, χ_{33}, χ_{34}, χ_{41}, χ_{42}, χ_{6}, deg), and scatter of potential energies within group (E_{pot}, kcal mol^{-1}), as given by molecular dynamics computations

Parameter	solv			
	N_{conf} 3	N_{conf} 39	N_{conf} 4	N_{conf} 5
ψ_{12}	175.7±2.8	170.5±5.8	170.9±3.4	175.4±2.1
ω_{12}	174.2±1.0	176.2±2.4	174.1±2.3	179.0±0.8
φ_{12}	94.3±6.2	95.7±6.1	93.4±6.6	93.6±3.4
ψ_{23}	114.3±2.6	109.6±3.8	111.5±4.0	108.0±2.9
ω_{23}	–172.2±4.2	176.4±2.0	–174.6±1.6	176.8±1.7
φ_{23}	–87.8±5.2	–79.9±5.5	–85.3±4.6	–81.6±3.6
ψ_{34}	141.9±2.1	134.3±4.8	139.4±1.4	128.5±2.8
ω_{34}	159.6±2.5	156.0±4.3	150.4±1.9	152.8±1.3
φ_{34}	–109.6±4.2	–95.8±5.1	–87.4±4.3	–83.4±5.0
ψ_{45}	132.9±1.1	128.6±3.3	139.6±4.3	125.5±2.9
ω_{45}	175.6±0.9	175.9±2.2	164.8±3.9	173.9±2.9
φ_{45}	–117.6±2.1	–115.9±5.5	–118.3±4.3	–116.5±2.2
ψ_{56}	136.5±1.4	131.4±4.6	138.8±0.8	129.2±3.4
ω_{56}	166.6±1.2	168.1±3.0	165.7±3.0	169.7±1.8
φ_{56}	–114.1±2.2	–105.3±3.0	–112.6±2.0	–107.1±5.1
χ_{31}	–93.1±4.0	–72.6±5.2	–77.5±8.7	–66.9±3.4
χ_{32}	176.8±2.1	–170.7±4.3	177.7±1.3	–173.1±4.4
χ_{33}	146.7±3.4	180±5	123.7±6.8	175.7±1.9
χ_{34}	60.9±1.4	–57.9±5.6	64.1±7.0	–61.6±4.0
χ_{41}	–162.8±5.2	–165.1±3.9	165.3±2.6	165.4±4.3
χ_{42}	–71.0±7.1	–73.0±7.1	–175.1±4.1	180±2
χ_{6}	–75.1±2.6	–77.4±2.7	–75.4±3.2	–76.9±4.3
E_{pot}	–74.90 to –80.33	–76.84 to –88.42	–79.57 to –85.57	–82.45 to –87.55

Parameter	desolv					dyn
	N_{conf} 6	N_{conf} 27	N_{conf} 6	N_{conf} 5	N_{conf} 35	
ψ_{12}	–170.2±1.0	–172.3±2.3	–172.3±1.7	180±2	–174.0±1.0	166.6±5.8
ω_{12}	179.5±0.4	174.3±0.8	174.1±1.1	–174.1±0.7	174.6±1.2	172.2±5.1
φ_{12}	75.4±1.1	52.8±1.1	50.9±1.8	73.5±1.2	52.6±1.8	91.5±7.2
ψ_{23}	176.8±1.4	–138.8±3.3	–136.2±1.2	168.7±1.2	–143.2±1.4	115.4±6.9
ω_{23}	177.9±0.4	169.1±1.7	170.0±1.1	–179.2±0.5	168.8±1.1	180±10
φ_{23}	–161.5±5.0	–142.2±1.8	–143.6±1.5	–172.2±0.9	–139.5±0.8	–87.8±6.8
ψ_{34}	103.0±2.5	175.5±2.0	177.1±1.6	83.8±2.4	178.2±1.4	141.9±7.3
ω_{34}	176.8±1.5	162.4±2.0	159.6±1.9	180±2	164.6±1.2	155.9±6.4
φ_{34}	–65.0±1.5	–88.2±2.7	–88.1±4.1	–58.4±1.6	–84.0±0.8	–93.0±8.1
ψ_{45}	147.9±1.9	142.6±2.2	145.4±1.7	143.1±2.1	134.7±2.6	147.7±9.1
ω_{45}	166.3±0.8	168.3±2.9	171.2±2.7	159.8±1.5	162.3±0.7	169.7±6.5
φ_{45}	–142.0±1.6	–138.9±3.6	–139.4±6.1	–141.3±1.9	–143.2±1.4	–125.3±7.8
ψ_{56}	–173.8±0.6	–166.2±4.5	–60.0±7.3	–174.9±0.6	178.7±1.4	129.9±6.7
ω_{56}	172.3±1.5	171.5±1.4	170.9±0.8	172.2±0.8	173.4±1.2	166.5±4.5

Table 3. (Contd.)

Parameter	desolv					dyn
	N_{conf} 6	N_{conf} 27	N_{conf} 6	N_{conf} 5	N_{conf} 35	
φ_{56}	–137.9 ± 1.1	–137.0 ± 1.8	–138.2 ± 1.6	–139.4 ± 1.2	–139.0 ± 1.4	–111.0 ± 5.9
χ_{31}	–101.4 ± 4.8	–71.6 ± 1.8	–68.5 ± 6.1	180 ± 2	–58.3 ± 0.6	–70.0 ± 9.2
χ_{32}	177.0 ± 0.7	–176.3 ± 1.8	–174.6 ± 1.5	–175.6 ± 0.3	–178.8 ± 0.4	180 ± 10
χ_{33}	167.9 ± 4.4	–166.2 ± 3.6	167.7 ± 1.1	180 ± 2	57.1 ± 0.8	–
χ_{34}	–72.0 ± 1.4	–67.3 ± 1.4	–65.0 ± 4.3	73.1 ± 1.0	176.6 ± 1.1	–
χ_{41}	–175.2 ± 1.4	180 ± 3	180 ± 2	–173.0 ± 1.1	–174.0 ± 1.2	–
χ_{42}	–97.1 ± 0.3	–94.2 ± 1.0	–175.9 ± 1.4	–176.3 ± 0.5	–174.0 ± 0.8	–
χ_6	–71.2 ± 0.3	–72.6 ± 1.0	–73.0 ± 1.0	–70.5 ± 1.0	–72.1 ± 0.7	–73.8 ± 8.1
E_{pot}	–125.50 to –125.74	–131.63 to –132.08	–133.37 to –133.61	–133.54 to –133.58	–136.05 to –136.15	–

either the amino group of the Lys^3 side chain or the hydroxy group of Thr^6. According the computation results, these groups both are sterically accessible. It thus can be suggested that the hydrogen bonding involves only one of these functional groups, since they are 10 Å apart and reside on different sides of the skeleton chain.

EXPERIMENTAL

Reagents and amino acid derivatives purchased from Sigma Chemicals, Fisher Scientific, Aldrich Chemicals (USA) were used in the synthesis of peptides. Dimethylformamide was distilled in a

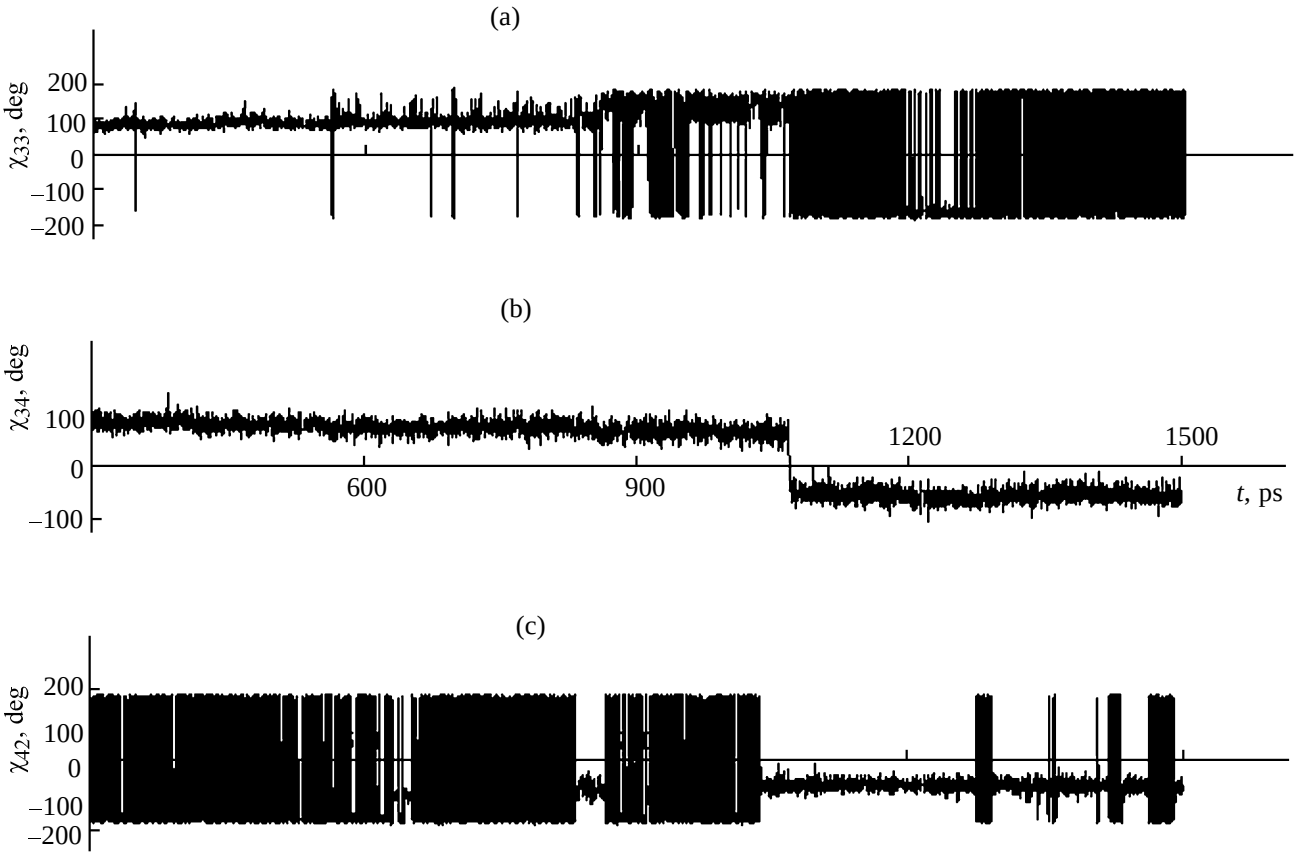

Fig. 4. Dependence of the (a) χ_{33}, (b) χ_{34}, and (c) χ_{42} dihedral angles in the H–Ala–*D*-Ala–Lys–Leu–Ala–Thr–NH_2 molecule on the time of molecular dynamics computations (*t*, ps).

vacuum and stored over 4 Å molecular sieves before use.

Desalination of peptides was performed on Sephadex G-15 (Pharmacia, Sweden). High-performance liquid chromatography was performed on a Waters-600E chromatograph (USA) using Vydac C-18 and Zorbax ODS-C-18 columns (4.6 × 250 mm) for analytical chromatography and Vydac C-18 (22 × 250 mm) and Delta Pak-C-18 columns (19 × 300 mm) for preparative chromatography. Hydrolysis of peptides was performed in 6 N HCl at 110°C for 24 h. Amino acid analysis was performed on a Microtechna T-339M amino acid analyzer (Czechia).

Solid-phase synthesis of peptides was performed on a poly(methylbenzhydrylamine) support (amino groups content 0.55 mmol g^{-1} [14]) on an 0.25 mmol scale using an NPS-4000 semiautomatic peptide sequencer (Neosystem, France). The polypeptide chain was elongated using the following protocol for each synthetic cycle (the solvent consumption in each stage was 10 ml): (1) CH_2Cl_2 (1 × 1 min); (2) 50% trifluoroacetic acid in CH_2Cl_2 (1 × 1 min); (3) 50% trifluoroacetic acid in CH_2Cl_2 (1 × 30 min); (4) CH_2Cl_2 (2 flow-up washings); (5) CH_2Cl_2 (2 × 1 min); (6) DMF (1 × 1 min); (7) 5% triethylamine in DMF (1 × 1 min); (8) 5% triethylamine in DMF (1 × 2 min); (9) DMF (3 × 1 min); (10) 3 equiv of activated BOC amino acid (2 h); (11) DMF (2 × 1 min); and (12) CH_2Cl_2 (1 × 1 min).

Preactivation of amino acids. To a solution of 3 equiv of BOC amino acid in 2 ml of DMF we added 0.75 ml of 1 M HOBu in DMF and, after cooling to 0°C, 3 equiv of diisopropylcarbodiimide. The reaction mixture was stirred at 0°C for 25 min. Acylation progress was followed by the ninhydrin test applied after operation 12 of the synthetic protocol [15]. At a positive test, the condensation cycle (operations 6–12) was repeated. Cleavage of peptide from polymer backbone with simultaneous deblocking was performed in the following way. A 2 : 1 mixture of thioanisole and ethanedithiol, 0.75 ml, was added to 0.5 g of the peptidyl polymer. The reaction mixture was magnetically stirred for 10 min, cooled to 0°C, and 5 ml of CF_3COOH was added. After 10-min magnetic stirring, 0.5 ml of trifluoromethanesulfonic acid was added dropwise, cooling was discontinued, and the reaction mixture was stirred for 2 h at room temperature, diluted with 200 ml of a cold diethyl ether, and the precipitate was filtered off. Peptide was separated from polymer by dissolution in CF_3COOH and then precipitated again with 200 ml of ether. The precipitate was filtered off, washed with ether, and dried in a vacuum. Peptide was desalinated on a column of Sephadex G-15 (1.9 × 110 cm) in 50% acetic acid and then purified with reversed-phase HPLC in a gradient of acetonitrile in 0.1% CF_3COOH, flow rate 10 ml min^{-1}, detection wavelength 229 nm.

The synthesized peptides were characterized by analytical HPLC and amino acid analysis. The HPLC analysis was performed at a gradient of acetonitrile in 0.1% CF_3COOH (from 5 to 30% in 25 min), flow rate 1 ml min^{-1}, detection wavelength 229 nm. The peptides all had correct amino acid compositions.

REFERENCES

1. Rapaka, R.S., Renugopalakrishnan, V., Goehl, T.J., and Collins, B.J., *Life Sci.*, 1986, vol. 39, no. 9, p. 837.
2. Pellequer, J.-L., Westhof, E., and Regenmortel, M.H.V. van, *Peptide Antigens: A Practical Approach*, Wisdom, G.B., Ed., Oxford, 1994, p. 7.
3. Monticelli, L., Mammi, S., and Mierke D.F., *Biophys. Chem.*, 2002, vol. 95, no. 2, p. 165.
4. Fu, P., Layfield, S., Ferraro, T., Tomiyama, H., Hutson, J., Otvos, L., Jr., Tregear, G.W., Bathgate, R.A., and Wade, J.D., *J. Pept. Res.*, 2004, vol. 63, no. 2, p. 91.
5. Epand, R.M., Stahl, G.L., and Orlowski, R.C., *Int. J. Pept. Prot. Res.*, 1986, vol. 27, p. 501.
6. Otani, M., Yamauchi, H., Meguro, T., Kitazawa, S., Watanabe, S., and Orimo, H., *J. Biochem.*, 1976, vol. 79, no. 2, p. 345.
7. Braga, P.C., *Agents Actions*, 1994, vol. 41, nos. 3–4, p. 121.
8. Epand, R.M., Epand, R.F., and Orlowski, R.C., *Int. J. Pept. Prot. Res.*, 1985, vol. 28, p. 105.
9. *HYPERCHEM Professional Release 5.1 (Demonstration Version), A Molecular Visualization and Simulation Software Package*, Geinesville: Hypercube, 1998.
10. Weiner, S.J., Kollman, P.A., Nguyen, D.T., and Case, D.A., *J. Comput. Chem.*, 1986, vol. 7, no. 2, p. 230.
11. Jorgensen, W.L., Chandrasekhas, J., Madura, J.D., Impey, R.W., and Klein, M.L., *J. Chem. Phys.*, 1983, vol. 79, no. 2, p. 926.
12. Kendrew, J.C., Klyne, W., Lifson, S., Miyazawa, T., Nemethy, G., Phillips, D.C., Ramachandran, G.N., and Scheraga, H.A., *Arch. Biochem. Biophys.*, 1971, vol. 145, no. 1, p. 405.
13. Vlasov, G.P., Glushenkova, V.R., Glynskaja, O.V., and Kotin, A.M., in *Chemistry of Peptides and Proteins*, Berlin: Walter de Gruyter, 1989, vol. 4, p. 89.
14. *The Peptides, Analysis, Synthesis, Biology*, Undenfriend, S. and Meienhofer, J., Eds., London: Academic, 1987, vol. 9.
15. Kaiser, E., Colescott, R.L., Bossinger, C.D., and Cook, P.I., *Anal. Biochem.*, 1970, vol. 34, p. 595.